SOLAR LIMB DARKENING 1986–1990 (λλ303 TO 1099 nm)

HEINZ NECKEL
Hamburger Sternwarte, Hamburg-Bergedorf, Germany

and

DIETRICH LABS
Landessternwarte Königstuhl, Heidelberg, Germany

(Received 2 August, 1993; in revised form 12 April, 1994)

Abstract. The Sun's limb darkening was observed repeatedly between the 1986 minimum and the 1990 maximum of solar activity. *Systematic* variations, which could depend either on the momentary activity and/or the phase in the solar cycle, were *not* detectable, either at continuum wavelengths or in two broad-band spectral intervals. Completely *irregular* variations, which concern not only individual, successive scans (due to granulation, etc.), but also the *daily* and *seasonal averages*, are usually less than 1%, but can reach occasionally 2% or even more. Minor *east–west asymmetries* even in the seasonal means seem to be well established, mainly for $\lambda < 400$ nm. The *final, mean* limb-darkening coefficients agree basically with those published by Pierce and Slaughter (1977) and Pierce, Slaughter, and Weinberger (1977), but show a much lower scatter when plotted against wavelength.

1. Introduction

Favoured by new technology and the corresponding increase in precision of solar radiation measurements in the last two decades the search for variations of the solar global radiation output has become an important – and promising – field in solar physics. E.g., the *total solar irradiance* (solar constant) is monitored continuously from space (on Nimbus-7 and SMM satellites) since 1978. It is now known to vary systematically within a solar cycle by about 0.15% and to exhibit short-term fluctuations with peak-to-peak amplitudes of up to 0.3% (see, e.g., Fröhlich, 1994). The *spectral irradiance* in the UV, visible and infrared have observed repeatedly since 1983 on special space missions (SPACELAB 1 and 2, UARS, ATLAS, EURECA). However, these observations have not provided yet definitive results about the true amplitudes of possible variations (see, e.g., Brückner *et al.*, 1994; Rottman *et al.*, 1994; and Thuillier *et al.*, 1994). Even the Sun's *spectral type* was observed repeatedly during the rising phase of cycle 22 and searched for possible variations. According to Keenan (1991), no changes could be detected between August 1988 and October 1990.

Our observations of the *limb darkening*, which were made between early June 1986 and late June 1990, were intended to supplement the observations quoted above. The first plans for the observing program were made in the early 1980's, when the magnitudes of possible variations in the Sun's radiative output were still rather unknown quantities. It should be noted that at that time some

Solar Physics **153:** 91–114, 1994.

observers explained major differences between different irradiance data (mainly below 400 nm) in terms of solar variability (e.g., Heath and Thekaekara, 1977: about 20% at 300 nm between the minimum and maximum of the solar cycle). Clearly, such large variations would have had their origin in changes of the structure of the solar photosphere, which should have been detectable also in the limb darkening.

The main result of our observations is the confirmation that the limb darkening did *not* show any detectable *systematic* differences between the 1986 minimum and the 1990 maximum of solar activity. Even more, our results agree very closely with the earlier measurements of Pierce and Slaughter (1977, hereafter 'PS') and of Pierce, Slaughter, and Weinberger (1977, 'PSW'). The main difference between their and our observations is the internal consistency: when plotted against wavelength, our final, mean data show a significantly lower scatter (factor 3!) than the PS- and PSW-data (presumably a result of limb-darkening variability, see below).

A secondary result is the information (from 5664 center-to-limb profiles), to what extent the normal limb-darkening scans (more precisely: 5th-order polynomials in $\cos\theta$ fitted to the observations) may *vary* from scan to scan, day to day, and season to season, due to all types of variable photospheric phenomena (granulation, oscillations, etc.).

2. Observations

Like the observations by PS and PSW, our observations were made at the National Solar Observatory/Kitt Peak, utilizing the McMath Solar Telescope and the large vertical spectrograph. Since also electronic equipment, observing procedure ('sampling the spectrometer output as the image drifts by diurnal motion across the entrance aperture'), and data reduction were very similar, for most of the relevant details we can refer to the PS paper (but compare also Neckel and Labs, 1984).

Reliable data could be obtained in seven observing seasons, of which four were in late June/early July, when the position angle of the Sun's rotation axis is around zero and the solar diameter defined by diurnal motion is least affected by active regions (1987–1990). The first season was in early June 1986, near activity minimum, two other seasons were in fall 1989 and spring 1990, when the position angle of the axis had its extreme values.

In 1986 and 1987 the observations included 30 continuum wavelengths from 303.3 to 1098.9 nm, which had been observed also by PS or PSW. Since June 1988 the number of wavelengths was drastically reduced to six (329.9 to 1046.7 nm). At that time we added to the main (spectrograph) channel two 'filter channels', which recorded the limb-darkening profiles in two fixed spectral bands almost simultaneously (offset in time ± 6 s). These bands were centered at 386.1 and 424.4 nm and had bandwidths of 6.1 and 7.9 nm (FWHM), respectively. The reason for this change was the existence of short-term variations and east–west asymmetries, which we found first in some scans obtained in 1986, and than also

in earlier observations (April 1981) by Neckel and Labs (1984) of the center-to-limb variation of 20 Å wide spectral bands (Neckel and Labs, 1987; compare also the criticisms by Foukal, 1989 and Elste, 1990, and the replies by Neckel and Labs, 1989, 1990). The first ('CN') filter channel includes the strong, temperature-sensitive CN absorption bands near 385 nm. This includes that spectral region which showed in 1981 the largest variations and asymmetries. The other one ('WL') includes mainly weak lines.

The following compilation presents further relevant instrumental and observational data (for more detailed information about telescope and spectrograph we refer to Pierce, 1964):

Diameter and focal distance of the main telescope mirror: 152/8246 cm or – since 1989 – 159/8693 cm; corresponding scale in focal plane: 2.50″ mm^{-1} or 2.37″ mm^{-1}, respectively.

Height of all three entrance slits: 10 mm. Width of entrance and spectrograph exit slits: 0.2 mm.

Bandwidth: from 0.015 Å at 303 nm (grating order 9) to 0.07 Å at 1099 nm (grating order 2); spectrograph used in double pass.

Detectors for spectrograph channel: multiplier EMI 9750 QB (bi-alkali cathode) for $\lambda < 550$ nm and silicon photodiode PIN 20 Å for $\lambda > 500$ nm. Photomultipliers for filter channels: EMI 9624.

All detector outputs were fed to pre-amplifiers and finally digitized at 1 kHz. Either 63 (1986/87) or 64 (1988–90) successive digitizations were summed by an on-line computer and each sum (= one data element or pixel) was recorded on magnetic tape. 4096 pixels covered one drift curve.

Resolution along the drift curve: 0.88″ $pixel^{-1}$ in summer seasons, 0.96″ $pixel^{-1}$ in spring and fall.

Usual arrangement of drift curve: dark signal (≈75 pixels) – 'short sky' (≈250 pixels) – Sun (≈2175 pixels in 1986/87, ≈2135 pixels in June/July 1988–1990, ≈2010 pixels in October 1989 and March 1990) – 'long sky' (between 1500 and 1700 pixels) – dark signal (≈75 pixels).

Disk center signal: usually between 20 000 and 30 000 ADU (analog-digital units; maximum value: 32767).

'Sky' signal at $\lambda = 520$ nm, 100″ from the limb (mainly light scattered from heliostat mirror!): between 0.11% (1986, after mirrors were aluminized) and 0.55% (1987) of disk center signal (all data in good agreement with results of Pierce, 1990).

Searching for any real, but – if present at all – presumably only weak variations in the course of many years requires the greatest possible precautions to reduce as far as possible any fictitious variations simulated by the instrumental equipment. In particular this requirement holds also for unexpected east–west asymmetries and short-term variations. The following points should be mentioned explicitly:

(1) Every morning the telescope mirrors wer carefully (re-)collimated, applying Kitt Peak standard rules.

(2) Light scattered or reflected from structural parts in the telescope tunnel was excluded by an orange filter foil (non-transparent for $\lambda < 500$ nm) in the window between the tunnel and observing room.

(3) The $\sim 90°$ angle between slit(s) and east–west driftline was kept constant within $0.2°$.

(4) The center of the solar disk passed the slit center(s) usually within less than $1''$.

(5) The predisperser was always set to the center of its flat transmission maximum.

(6) The wavelength settings were made with disk center light at carefully selected continuum positions, which showed a minimum of intensity variation within the limits defined by the rotational limb-to-limb wavelength shift ($\Delta\lambda/\lambda = 1.3 \times 10^{-5}$ or 0.04 Å at 303 nm). This procedure explains some minor differences between our wavelength positions and those of PS.

(7) Only carefully selected photomultipliers without any detectable hysteresis effects were used.

(8) For the spectrograph channel, also the linearity of the electronics was very precisely tested. Minor, but well-founded deviations from linearity (<0.1% of maximum signal) were taken into account.

3. Data Reduction

3.1. Definition of Limb Positions

The limb positions were determined in two steps:

(1) Following PS and PSW, we approximated the limb positions by the positions of the steepest gradients or 'limb inflection points' (for the precise procedure, see Neckel and Labs, 1984). The average deviations of the resulting semi-diameters from the values given in the *Nautical Alamanac* ranged from $\sim -0.5''$ at λ311 nm to $\sim -0.1''$ at λ445 nm, and scattered between $-0.07''$ and $+0.02''$ at longer wavelengths. According to one-dimensional integrations across the limb (using PS coefficients to represent the true limb darkening), these characteristics correspond to a seeing of $\sim 3''$ (FWHM $= 5''$), which is a reasonable value for day-time observations on Kitt Peak. Because of this almost perfect agreement with the *Alamanac* value, we determined improved limb positions by means of step 2:

(2) The final limb positions were obtained from *improved* positions of the disk center and the *Almanac* values of the semi-diameter. The improved center positions were *not* based on the *maxima* of the derivative curve of the observed limb profile (= inflection points!), but instead on their much better defined *centers of gravity* (derived from 12 successive pixels in the limb regions). Thereby, the mean errors of the disk center positions could be reduced to values ranging from $0.6''$ at λ311 nm to $0.4''$ at λ1047 nm.

The conversion from pixel units into arc sec (and *vice versa*) was made using the relation

$$1'' = \Delta T_{\text{Sun}}/(360 \times T_{\text{pixel}} \cos\delta)\ \text{pixel}\ , \tag{1}$$

where ΔT_{Sun} denotes the time (in hours) between two successive meridian passages of the Sun, T_{pixel} is the integration time of 1 pixel (0.063 or 0.064 s), and δ is the Sun's declination.

Our second step neglected of course the dependency of the limb positions on wavelength, but this is small in comparison to the seeing effects, at least at continuum wavelengths (according to data given by Unsöld, 1955, maximum deviations from mean value $\approx\pm 0.07''$ near 350 nm (−) and 800 nm (+)). However, due to the inclusion of chromospheric radiation at the extreme limb regions, the CN channel yielded semi-diameters which were $\sim 0.5''$ *larger* than the *Almanac* values.

3.2. Least-square fits of 5th-order polynomials

From four types of functions which were fitted by PS(W) to observed limb-darkening profiles, 5th-order polynomials in $\mu = \cos\theta$ were found to provide the best representation. For our reduction of individual scans we adopted that optimum solution. However, in the following details our procedure differed from that of PS(W):

(1) We did not form normal points, but fitted the polynomials – in principle – to all of the about 1000 signals along each radius (each signal got its μ according to its position between disk center and final limb position).

(2) To eliminate seeing effects near the limb, the signals within $7''$ from the limb were excluded.

(3) The fits were made to the *normalized* signals (corrected for linearity and dark signal, divided by the maximum signal), but these were *not* corrected for scattered light. If such corrections were desirable, they were applied to the resulting polynomials, and then new fits were made (see Section 3.3).

(4) For each radius the least-square fits were repeated as long as there were any data with residuals exceeding the standard deviation σ by a factor larger than 3, with those points being excluded. This simple procedure served mainly to eliminate regions with spots and/or faculae, which on some days of the later observing periods crossed one or the other radius.

Naturally, east and west polynomials did not yield precisely the same disk center value. In order not to introduce systematic scale differences between both polynomials, they were not individually normalized to yield exactly 1.0 at disk center, but were both scaled with the one factor which gave unity for the east–west *mean* polynomial. Therefore, the final disk center values were either $1 + \epsilon$ (west polynomial) or $1 - \epsilon$ (east polynomial), with $|\epsilon|$ being usually less than 0.0015.

For the five summer seasons (no activity on the scanned diameter), the average number of signals excluded along one radius was 10, the maximum number 38. Typical values for the final one-pixel standard deviation σ_{final} (granulation) are, for these seasons, 0.8% at 330 nm, 0.4% at 1047 nm, 1.0% for the CN- and 0.7% for the WL-channel (% of disk center intensity). However, if active regions crossed

the radius, the number of excluded signals could be as large as 79 (October 10, 1989) and 116 (March 25, 1990). At such times also σ_{final} was clearly larger in the filter channels, in particular in the CN-channel (compare Section 5, Figure 9: σ_P).

3.3. Corrections for Scattered Light

Following PS, we consider *scattered light* as that portion of the *stray light* which is '*...scattered at angles from 0° to 90° by aerosols, dust in the atmosphere, and by diffraction as well as by dirty, scratched and generally imperfect optics...*'. So, we do not consider special corrections for seeing (or *blurring*), which '*...refers to displacements caused by refractive index inhomogeneities in the Earth's atmosphere and is generally limited to small angles – 0 to 10″...*'.

With a seeing parameter of 3″ (FWHM = 5″) and the limb-darkening profile for $\lambda = 320$ nm, at 7″ from the limb, the due intensity corrections get below 0.15% of the disk center intensity. This justifies our procedure to 'correct' the limb profile for *seeing*: to exclude the seven signals nearest to the limb and to accept the limb 'restoration', which resulted from the extrapolation of the polynomials.

For an estimate of the influence of *scattered* light on the limb-darkening profiles, for each scan the 'sky' intensities were determined at seven distances from the limb (10, 20, 50, ..., 1000″). The dependence of these data on the treatment of mirror surfaces (washing or aluminization) confirmed very clearly that the scattered light is mainly produced on the surface of the heliostat mirror. Therefore, the scattered light was treated as (a) originating in one, infinitely extended dust layer, and (b) being time-independent within one observing season (usually 7 successive days).

The actual corrections for scattered light, $\Delta I(r) = I_{\text{true}}(r) - I_{\text{obs}}(r)$, follow from

$$I_{\text{obs}}(r) = I_{\text{true}}(r)\,[1 - S(0)] + S(r)\,, \tag{2}$$

where r is the distance from the disk center (in arc sec), $I_{\text{true}}(r)$ is the true, $I_{\text{obs}}(r)$ is the observed intensity distribution [$I_{\text{obs}}(0) = I_{\text{true}}(0) = 1.0$], and $S(r)$ is the scattered light.

$S(r)$ follows from integration over the solar disk:

$$S(r) = 2\int_0^R \int_0^\pi I_{\text{true}}(x)\psi(\rho)x\,\mathrm{d}\phi\,\mathrm{d}x\,, \quad \rho = \rho(x, r, \phi)\,, \tag{3}$$

where ϕ is the angle at disk center between the directions towards scattering and receiving element, R is the solar semidiameter (in arc sec), and $\psi(\rho)$ is the scattering function

$$\psi(\rho) = A[\pi a^2 \exp(\rho^2/a^2)]^{-1} + B(m-1)\,[\pi b^2(1 + \rho^2/b^2)^m]^{-1}\,. \tag{4}$$

Here A, a, B, b, and m are the scattering parameters, which were determined by the trial and error method so that observed and computed 'sky' intensities ($I_{\text{obs}}(r)$

and $S(r)$ for $r > R$) agreed as well as possible (n.b.: A and B denote the fractions of light scattered by the first or second term, respectively; with $A + B = 1$ the integral of $\psi(\rho)$ over the whole sky ($\rho \rightarrow \infty$) becomes equal to 1). Except for m (constant = 1.1), these parameters changed from season to season and depended – of course – on the wavelength. In 1987, the year with the highest scattered light, they ranged between the following values, which include the shortest (303 nm) and longest (1099 nm) wavelengths, respectively: $0.022 \geq A \geq 0.004, 75'' \geq a \geq 50''$, $0.152 \geq B \geq 0.078, 250'' \leq b \leq 1150''$. At the local maximum at $\mu \approx 0.7$, the corresponding corrections varied from +0.20% (303 nm) to +0.04% (1099 nm), and at $\mu = 0.1$ ($5''$ from the limb) from −0.75% (303 nm) to −0.01% (1099 nm) of disk center intensity.

N.B.: Since the corrections $\Delta I(r)$ are small and do not vary significantly if the limb darkening is slightly altered, it was fully sufficient to use in Equation (3) for $I_{\text{true}}(r)$ the polynomials $I_{\text{obs}}(r)$ fitted to the *observed* profiles. The corrections were computed for and applied to 101 equidistant values ($0.00 \leq \sin\theta \leq 1.00$) of the 'observed polynomials', and then the 'true polynomials' were fitted to the 101 corrected data points.

4. Average Limb Darkening in 1986 and 1987

For the 30 wavelengths observed in 1986 and 1987 the coefficients $A_0 \ldots A_5$ of the final polynomials $P_5(\mu)$,

$$P_5(\mu) = A_0 + A_1\mu + A_2\mu^2 + A_3\mu^3 + A_4\mu^4 + A_5\mu^5\,, \quad \Sigma A_n = 1.0\,, \qquad (5)$$

are given in Table I. These data are the averages of the two seasonal means, both individually corrected for scattered light. The table includes also the numbers of scans (N_{86}, N_{87}) which yielded the averages, and the ratios of disk-averaged to disk-center intensities, F/I:

$$F/I = 2(A_0/2 + A_1/3 + A_2/4 + A_3/5 + A_4/6 + A_5/7)\,. \qquad (6)$$

A comparison of our results ('NL') with those of PS and PSW (Figure 1) reveals a significant difference in scatter: the ratios of the standard deviations (PS/NL and PSW/NL) with respect to smooth curves are 3 : 1! Actually, *our data display the coefficients of limb darkening as almost smooth functions of wavelength (except – of course – for the Balmer discontinuity), and allow very reliable fits of smooth and monotonic interpolation functions.*

Figure 2 displays the differences between NL and PS(W) polynomials as a function of θ. The dashed curves, added at eight wavelengths, demonstrate the estimated effects of scattered light. The variety of forms and features corresponds to the scatter found in Figure 1 for the PS(W) coefficients. The exceptionally large differences for λ303 nm are presumably due to the sensitivity to minor wavelength displacements caused by solar rotation (see point (6) at the end of Section 2). From

TABLE I

Coefficients of limb-darkening functions $P_5(\mu)$ (Equation (5)) (mean of 1986 and 1987 east-west averages, corrected for scattered light)

λ (nm)	N_{86}	N_{87}	A_0	A_1	A_2	A_3	A_4	A_5	F/I
303.327	13	12	0.08011	0.70695	0.49910	−0.31080	−0.02177	0.04642	0.6826
310.843	11	10	0.08160	0.71609	0.69685	−0.87703	0.47008	−0.08760	0.6883
320.468	13	12	0.08833	0.77285	0.65382	−1.04647	0.72921	−0.19775	0.6985
329.897*	17	9	0.09188	0.92459	0.19604	−0.39546	0.23599	−0.05303	0.7116
349.947	14	8	0.11012	1.02168	−0.10924	−0.00055	−0.08688	0.06487	0.7260
365.875	14	10	0.12828	1.04969	0.17482	−1.13371	1.23882	−0.45990	0.7445
374.086	12	10	0.12579	0.85402	0.54601	−1.15048	0.88928	−0.26462	0.7288
390.915	13	10	0.12995	0.91836	−0.07566	0.19149	−0.28712	0.12298	0.7204
401.970*	13	10	0.12323	1.08648	−0.43974	0.45912	−0.32759	0.09850	0.7303
416.319	14	7	0.12814	1.19947	−0.84407	1.07201	−0.79537	0.23982	0.7380
427.930	12	8	0.14249	1.28796	−1.19564	1.68603	−1.36658	0.44572	0.7495
443.885	15	8	0.16220	1.24893	−0.92165	0.89978	−0.50148	0.11220	0.7588
445.125*	13	8	0.15248	1.38517	−1.49615	1.99886	−1.48155	0.44119	0.7596
457.345	13	10	0.16604	1.38544	−1.52275	2.00232	−1.45969	0.42864	0.7651
477.427	13	8	0.19571	1.30551	−1.25845	1.50626	−1.05472	0.30570	0.7751
492.905	22	8	0.20924	1.30798	−1.20411	1.21505	−0.67196	0.14381	0.7823
519.930*	17	12	0.23695	1.29927	−1.28034	1.37760	−0.85054	0.21706	0.7925
541.760	12	12	0.26073	1.27428	−1.30352	1.47085	−0.96618	0.26384	0.8002
559.950	10	8	0.26892	1.34319	−1.58427	1.91271	−1.31350	0.37295	0.8061
579.880	13	8	0.28392	1.36896	−1.75998	2.22154	−1.56074	0.44630	0.8125
610.975	11	6	0.30854	1.36620	−1.83572	2.33221	−1.63082	0.45959	0.8221
640.970	14	6	0.33644	1.30590	−1.79238	2.45040	−1.89979	0.59943	0.8290
669.400*	14	6	0.34685	1.37539	−2.04425	2.70493	−1.94290	0.55999	0.8360
700.875	12	6	0.37885	1.25553	−1.70908	2.19647	−1.59554	0.47378	0.8434
748.710	14	8	0.40627	1.22842	−1.67877	2.05535	−1.39972	0.38845	0.8524
811.760	10	6	0.42977	1.25182	−1.85164	2.31949	−1.59101	0.44155	0.8621
869.600	10	6	0.45396	1.25101	−2.02958	2.75410	−2.02287	0.59338	0.8701
948.850	10	8	0.47855	1.19813	−1.86296	2.36939	−1.64367	0.46056	0.8773
1046.600*	11	8	0.49870	1.21429	−2.06976	2.80703	−2.05247	0.60221	0.8841
1098.950	9	8	0.51149	1.19354	−2.00174	2.66936	−1.94981	0.57715	0.8890

* mark the 6 wavelengths exclusively observed since 1988.

Figure 1 it is obvious that mainly the PS data suffered from this problem. The only *systematic* differences (PSW−NL $\approx$ 0.4%) are found for the six wavelengths $\lambda \geq 749$ nm, which all show a similar distribution over θ.

In Figure 3(a) we plotted the ratios F/I of disk-averaged to disk-center intensities, which follow from the data given in Table I, and the PSW ratios as well.

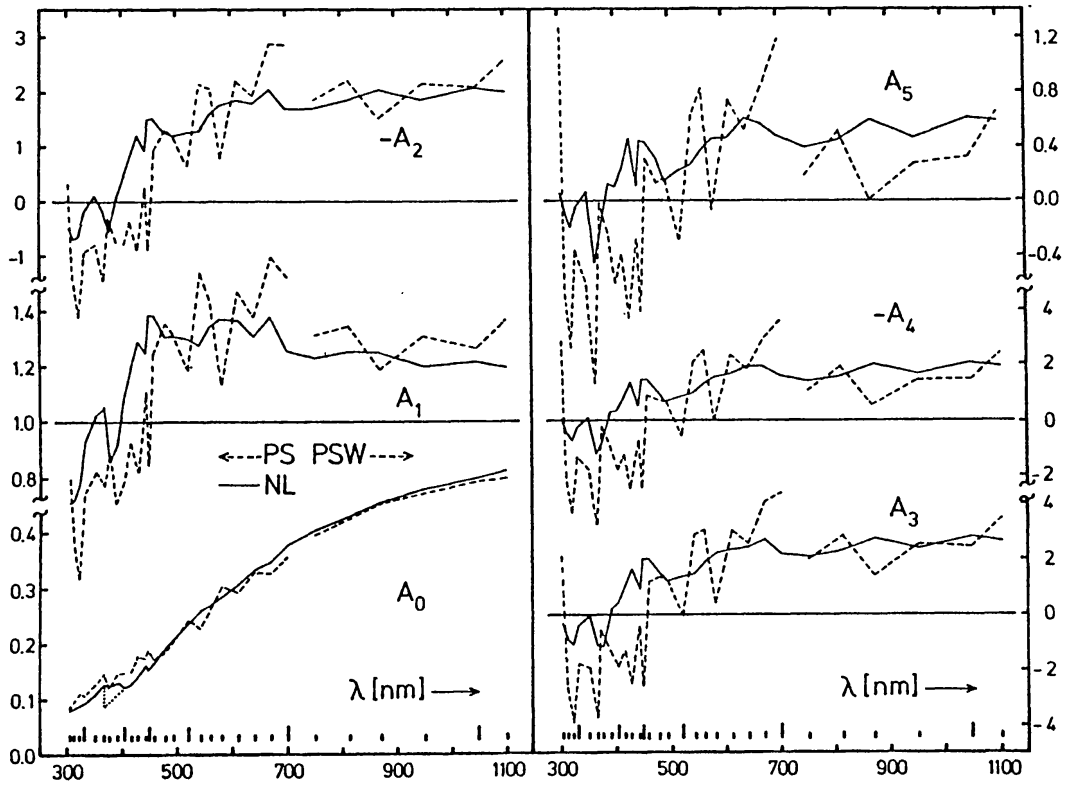

Fig. 1. Coefficients $A_0 \ldots A_5$ of 5th-order polynomials $P_5(\mu)$ from our Table I ('NL'), from Table IV of Pierce and Slaughter (1977, $\lambda \leq 701$ nm, 'PS') and from Table IV of Pierce, Slaughter, and Weinberger (1977, $\lambda \geq 749$ nm, 'PSW'). Markings at the bottom indicate observed wavelengths (longer dashes for the 6 wavelengths observed exclusively since 1988). In the A_0-plot, the dotted line marks the position of the Balmer 'jump'.

Figure 3(b) displays the corresponding differences PS–NL and PSW–NL, which are a convenient measure for the *average* intensity difference along the solar diameter. The PS–NL differences range between −0.002 and +0.002; on average they are close to zero. Systematic effects are not detectable (again: disregard the first value at λ303 nm). The PSW–NL differences show, of course, the systematic trend that was found already in Figure 2.

With respect to these systematic differences between PSW and NL data (≈0.4%), we do note that even larger differences (≈1%) were found by PSW, when they compared their first (1974/75) results for $740 \leq \lambda \leq 2402$ nm with observations of Allen (1976), which were obtained with the 75-cm aperture auxiliary system of the McMath Telescope for $\lambda \geq 1600$ nm. After '...further observations at the old wavelengths and by observations of many other new wavelengths...' (in spring 1976), they found '...that a discrepancy still exists, but is reduced...'. Since PSW suspected that the discrepancies could be '...related to short term changes in limb darkening...', they observed on one day for six hours the limb darkening at three wavelengths, and concluded from the results that '...there is no evidence from these observations for short-period changes in the limb darkening...'.

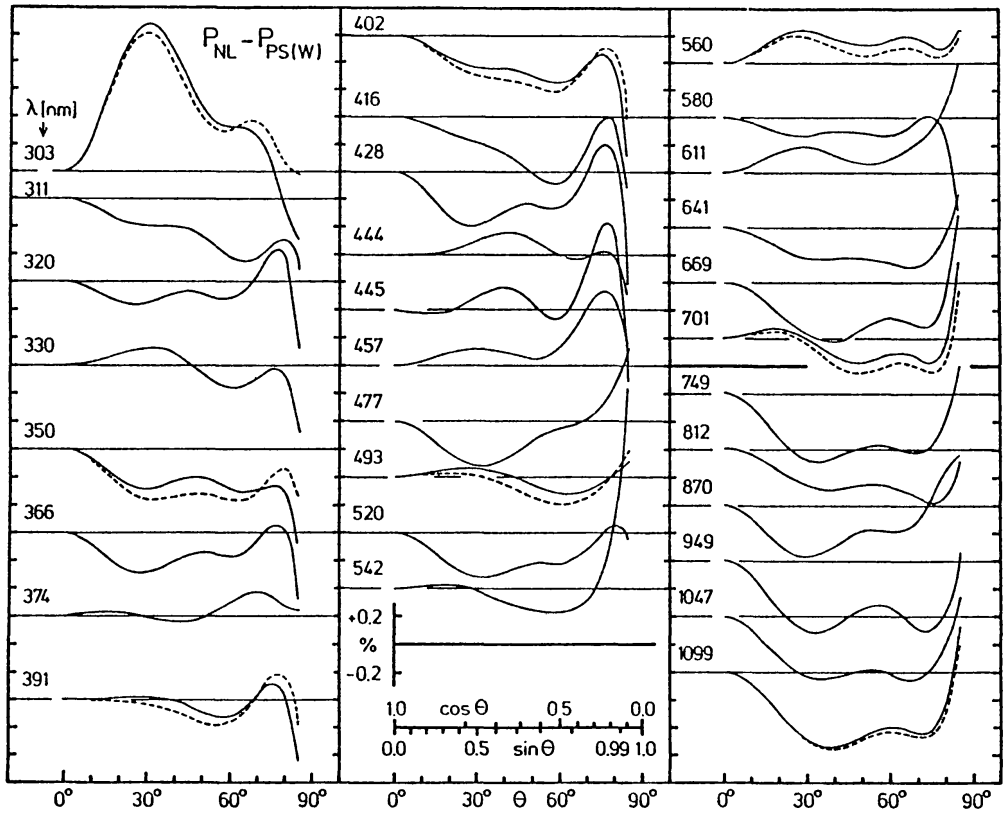

Fig. 2. Differences between 5th-order polynomials P_{NL} and $P_{PS(W)}$ as a function of θ ($\theta \leq 85°$, $\cos\theta \geq 0.087$; in % of disk center intensity). The 8 dashed curves concern NL-polynomials *not* corrected for scattered light.

We suppose that these differences – and the different scatter found in Figure 1 as well – result from 'quite normal' variations with time scales in the order of *days and weeks*. In this respect it should be noted that PS gathered their observations on 14 days within an 11-month period (March 1974 to January 1975), and the PSW observations extended over about 16 months. On the other hand, our data are averages from two 7-day periods. In Section 5 we present further observational details which seem to confirm this supposition.

5. Limb-Darkening Variations and East–West Asymmetries 1986–1990

5.1. Results for 30 wavelengths observed in 1986 and 1987

In Figure 3(c), the upper plot displays the average west-minus-east F/I-differences observed in 1986 and 1987. While these differences scatter for $\lambda \geq 402$ nm around the zero line within about ± 0.001, they are systematically below zero for $\lambda < 400$ nm. The similarity of this plot with the A_1-distribution in Figure 1 seems to indicate that these differences reflect a real east–west asymmetry of the solar limb darkening rather than instrumental imperfections. The lower plot reveals how closely in both years the *average* west-minus-east differences did agree.

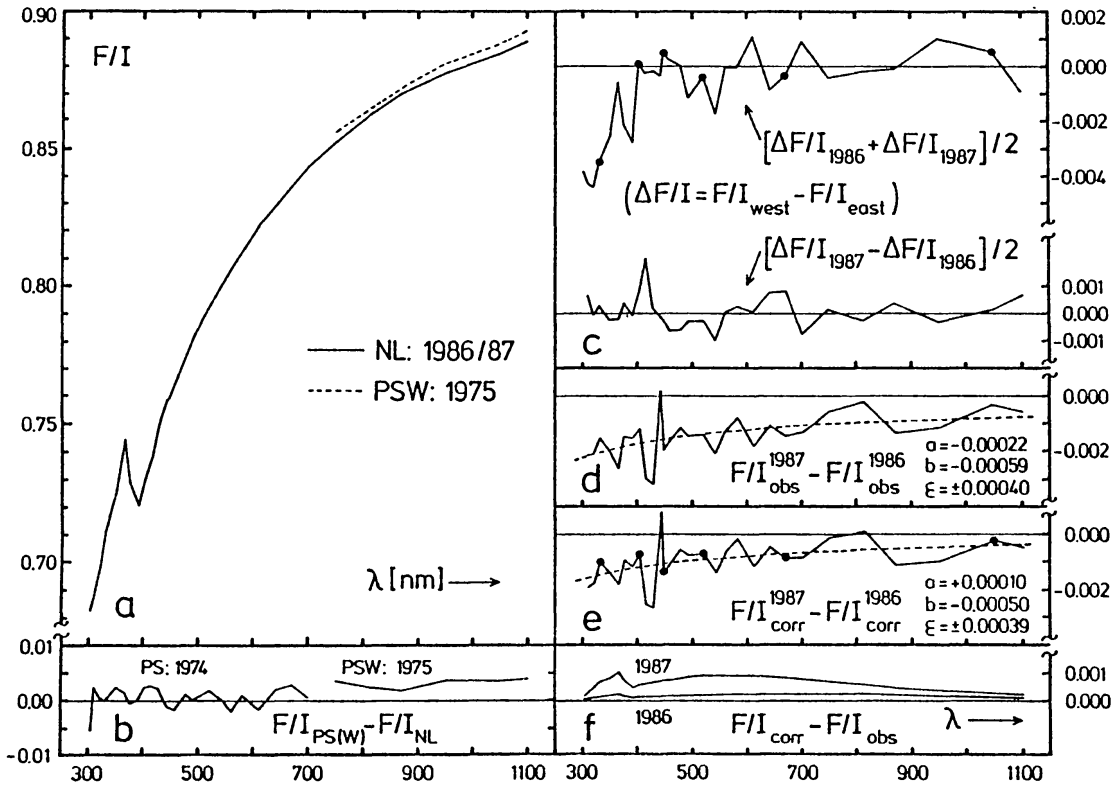

Fig. 3. (a) Ratios F/I of disk-averaged to disk-center intensity from 5th-order polynomials P_{NL} and P_{PSW}. (b) F/I-differences PS–NL and PSW–NL. (c) Differences $\Delta F/I = F/I_{west} - F/I_{east}$: mean values (1986+1987)/2 and half differences (1987–1986)/2. (d) Differences between 1987 and 1986 east–west averages before and (e) after correction for scattered light (dashed curves; least-square fits $\Delta F/I = a + b/\lambda$). (f) Differences between *corrected* and uncorrected ('*obs*erved') F/I ratios for the two seasons with minimum and maximum of scattered light. In (c) and (e), thick points mark those 6 wavelengths observed exclusively since 1988.

Further, Figure 3 shows the F/I differences between the 1987 and 1986 east–west averages, (d) before and (e) after being corrected for scattered light, and displays (f) the corrections for both years. Although the F/I differences are in the order of only 0.001, they nevertheless exhibit a clear dependence on wavelength, which is best approximated by a λ^{-1} law (dashed curves). Therefore we conclude again that the observed differences are not caused by instrumental effects, but do indicate a minor, real variation of solar limb darkening.

Comparing plots (b) and (e), the ratio of the ordinate scales (factor 5) should be taken into account: the scatter in the 1987–1986 differences is by a factor 3 lower than that in the PS(W)–NL differences! Of course, also the differences between the seasonal polynomial averages (not shown) are for most wavelengths significantly lower than the NL–PS(W) differences shown in Figure 2.

5.2. Results for six wavelengths observed from 1986 to 1990 (and for the two filter channels observed since 1988)

For the six continuum wavelengths observed exclusively since 1988, all results were related to the 1986–1987 east–west averages (Section 4 and Table I). In

order to include also the 1986–1987 results in this overall discussion, the 30 original wavelengths were assigned to six wavelength groups, which were then treated as concerning one of the final six wavelengths. For the two filter channels the reference polynomials are based on 237 scans, which were obtained partly in June/July 1989 (185 scans), partly in June 1990 (52 scans). These scans were selected so that the averages of the simultaneously observed continuum profiles agreed as closely as possible with the 1986–1987 averages. So, we suppose that all eight reference profiles represent as closely as possible the same physical state of the solar atmosphere.

N.B. The main purpose of the two filter channels was to insure that any observed variations were not caused by instrumental effects or by variable transparency of the Earth's atmosphere. Actually, almost all variations occur in the three channels (SP = spectrograph, CN, WL) with very similar patterns, but which differ in the details in a way which clearly indicates their solar origin. Of course, the three channels probe the temperatures, etc., in part at quite different *geometrical* depths. A second purpose was to get a better chance to detect any possible periodicities in the observable variations. In this respect the filter channels could not help: the variations appear to occur in a completely chaotic manner.

In the course of the reduction it became obvious that our seven observing seasons can be assigned to two categories: four seasons show *normal* and three seasons *exceptional* limb-darkening characteristics. Figures 4 and 5 demonstrate the differences by means of (1) the daily average deviations of the F/I ratios from their standard values defined above, which are plotted separately for the west and east polynomials, and (2) the corresponding seasonal east–west averages.

The two upper plots of Figure 4 should be compared with Figures 3(c) and 3(e); note that at 330 nm both plots show on all days nearly the same differences west–east (in the average 0.35% of the disk center intensity, first thick point in Figure 3(c)). The minor, systematic differences which concern all six wavelengths (the 1986 *seasonal* means appear 'too high', the 1987 means 'too low') reflect the facts that (1) both seasonal means are related to their averages, and (2) in 1987 all F/I ratios were lower than in 1986 (Figure 3(e)).

The differences between both categories are very obvious: they concern the size of the seasonal overall means of $\Delta F/I$, the order of magnitude of the day-to-day scatter of the daily means (west and east), and the size of the west-minus-east differences.

5.2.1. Seasons with 'Normal' Limb Darkening ('Normal Seasons')

In Figure 4 the following characteristics are found for all *continuum wavelengths*: (1) The lowest seasonal F/I averages were in 1987 (compare also Figure 3(e)). (2) The averages for 1989 and 1990 agree very closely with those observed in 1986 (maximum difference: 4×10^{-4}; one exception: λ669 nm in 1989). (3) The differences west-minus-east (at 330 nm) were (absolutely) largest near activity minimum (1986, 1987), clearly smaller but still noticeable in 1989, and vanished

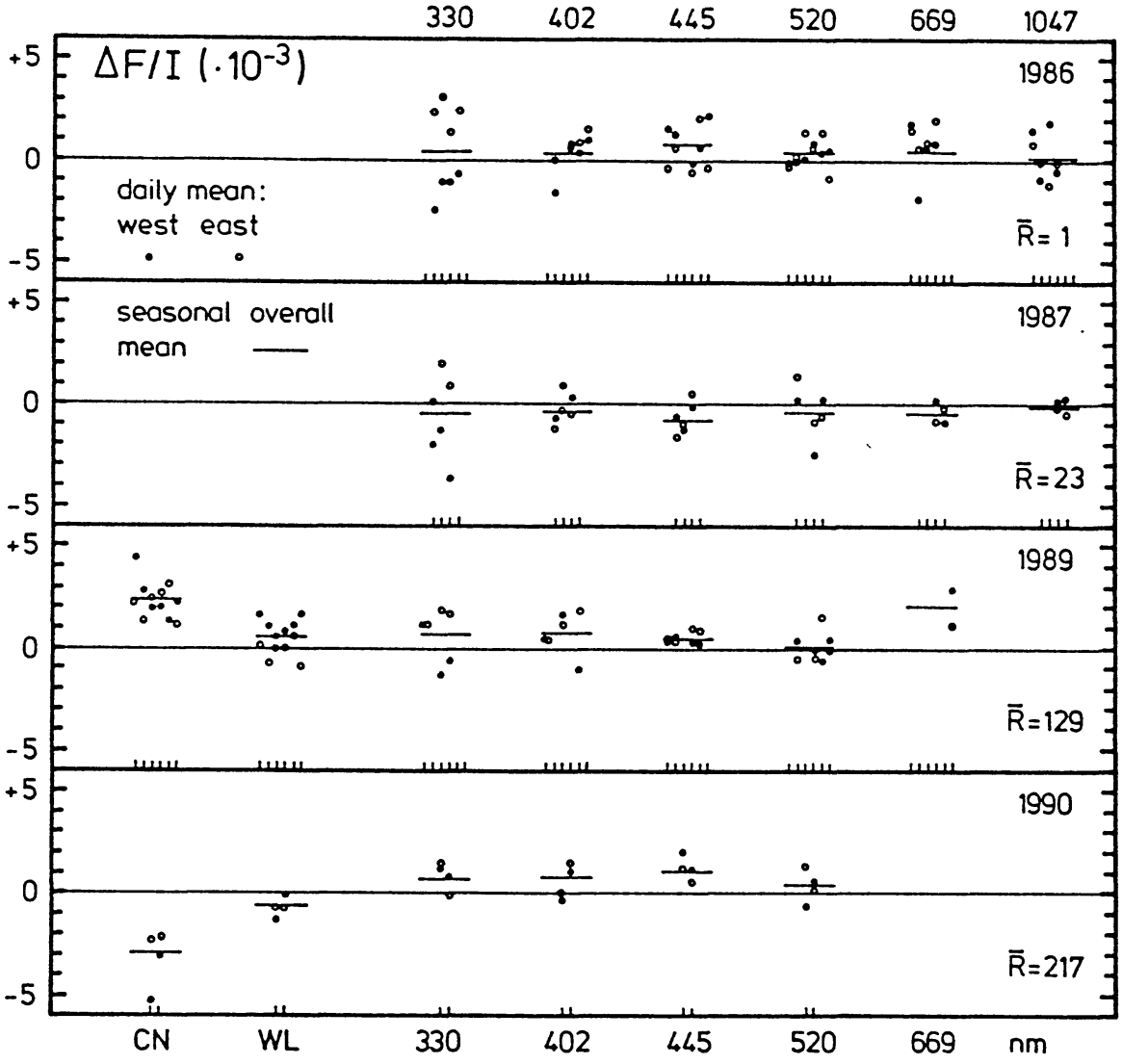

Fig. 4. Deviations $\Delta F/I$ from the reference values for (1) the daily western and eastern averages and (2) the overall seasonal means. Data at the bottom identify the filter channels and the observed continuum wavelengths. The plots refer to the four summer seasons (June/July) with 'normal' limb darkening. Vertical marks identify the consecutive observing days. The averages of the daily sunspot numbers, R, are given at the lower right.

in 1990, near activity maximum. Of course, due to the low number of seasons this trend is not well founded and may be accidental.

Concerning the two filter channels, we point to the following details: (1) In both channels, the 1989 seasonal F/I averages (based on 282 limb-to-limb scans) are higher than the 1990 averages (from 67 scans). (2) The CN difference is clearly larger than the WL difference. (3) The scatter of the daily averages is comparable in size to the scatter at continuum wavelengths. (4) The daily averages show either no (CN: 1989; WL: 1990) or only minor systematic west-minus-east differences (WL, 1989: west>east; CN, 1990: west<east).

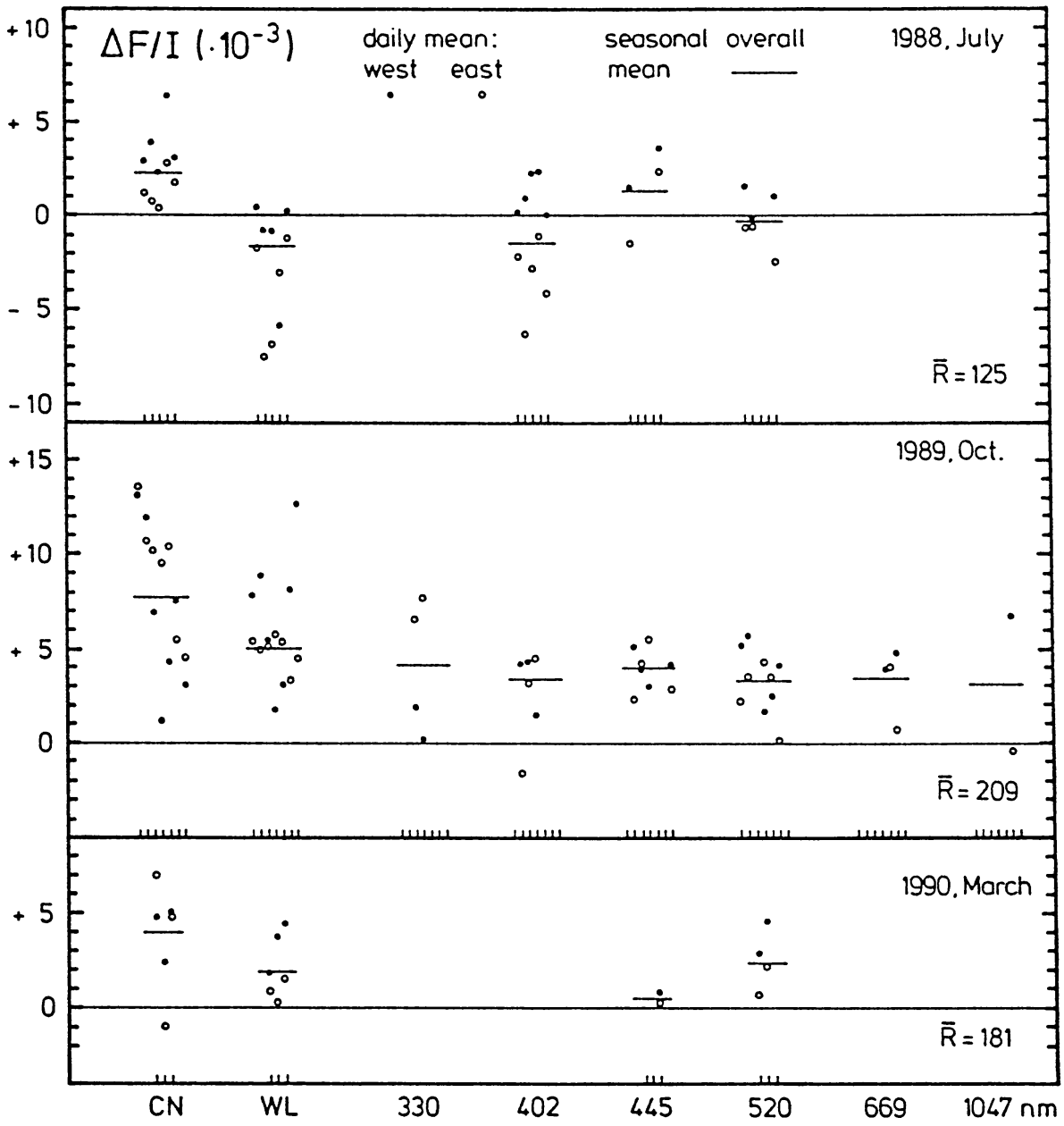

Fig. 5. Deviations $\Delta F/I$ from the reference values as in Figure 4, but for the three observing seasons with 'exceptional' limb darkening.

Figure 6 reveals that the close agreement between the 1989 and 1990 averages with the reference polynomials (average 1986–1987) actually concerns the whole intensity distribution between the limbs (except λ669 nm in 1989 and the CN channel).

From Figures 4 and 6 it seems to be evident that *in 'normal seasons' the solar limb darkening does not depend either on the phase within the activity cycle or on*

the momentary activity, as it may be measured, e.g., by the sunspot numbers (their seasonal averages are inserted in Figures 4 and 5).

Since the CN limb-to-limb profiles are strongly affected by the complex chromospheric structures, there is no need to analyze the CN-specific deviations from the reference. As pointed out before, we take the features observed in both filter channels just as a test-tool for the origin of limb-darkening peculiarities at continuum wavelengths. Nevertheless, the last five CN plots of Figure 6 are good for demonstrating a special characteristic of our data reduction: if we had normalized eastern and western polynomials separately to become unity at disk center, in all five plots the eastern polynomials would have agreed very closely with the reference polynomials; it seems that it is just the western polynomials which terminate at disk center at the 'wrong' intensity, which was in 1989 'too low', in 1990 'too high'. In this sense it was our special procedure to normalize eastern and western polynomials (see Section 3.2), which caused the eastern polynomials to get 'too high' (1989) or 'too low' (1990). On the other hand, separate normalization would have led to considerably larger (and totally wrong!) east–west differences. This effect may have contributed to the fact, that the asymmetries we had found in limb-to-limb scans of 20 Å wide spectral bands (Neckel and Labs, 1987) were – on average – larger than those revealed in this paper.

5.2.2. Seasons with 'Exceptional' Limb Darkening ('Exceptional Seasons')
From Figures 4 and 5 it is evident that in 'exceptional seasons' the following F/I data are clearly larger than their 'normal' values: (1) the deviations of the seasonal means from the reference values, (2) the day-to-day scatter of the daily means (west and east), and (3) the size of the west-minus-east differences. But also the signs of these differences need consideration: in all three exceptional seasons the western F/I ratios were mostly larger than the eastern ones, except for λ330 nm (opposite sign; the same one as in 1986, 1987, 1989) and for the CN channel (in 1989 and 1990, not in 1988).

Figures 7 and 8 display the corresponding difference $\Delta P(\theta)$. In Figure 7 one should note that in both seasons (1988 July, 1990 March) the maximum deviations in the channels SP and WL were of about the same size. This fact needs to be emphasized because of the different observing conditions: during the first season the observed diameter was near and parallel to the Sun's equator, the activity cycle was still at an early phase, the actual, global activity at a moderate level ($R \approx 125$), and there was no detectable activity near the observed diameter; during the other season the angle between the observed diameter and the Sun's equator was almost at its maximum (26°), the solar cycle was near its maximum phase, the actual activity was at a high level ($R \approx 180$), and on one of the three observing days (March 25) a large sunspot group near disk center and intense faculae near the western limb as well as at eastern longitudes crossed the observed diameter. This agreement indicates that our simple procedure to exclude active regions from the polynomial fits (see Section 3.2) worked sufficiently well, and that the limb-

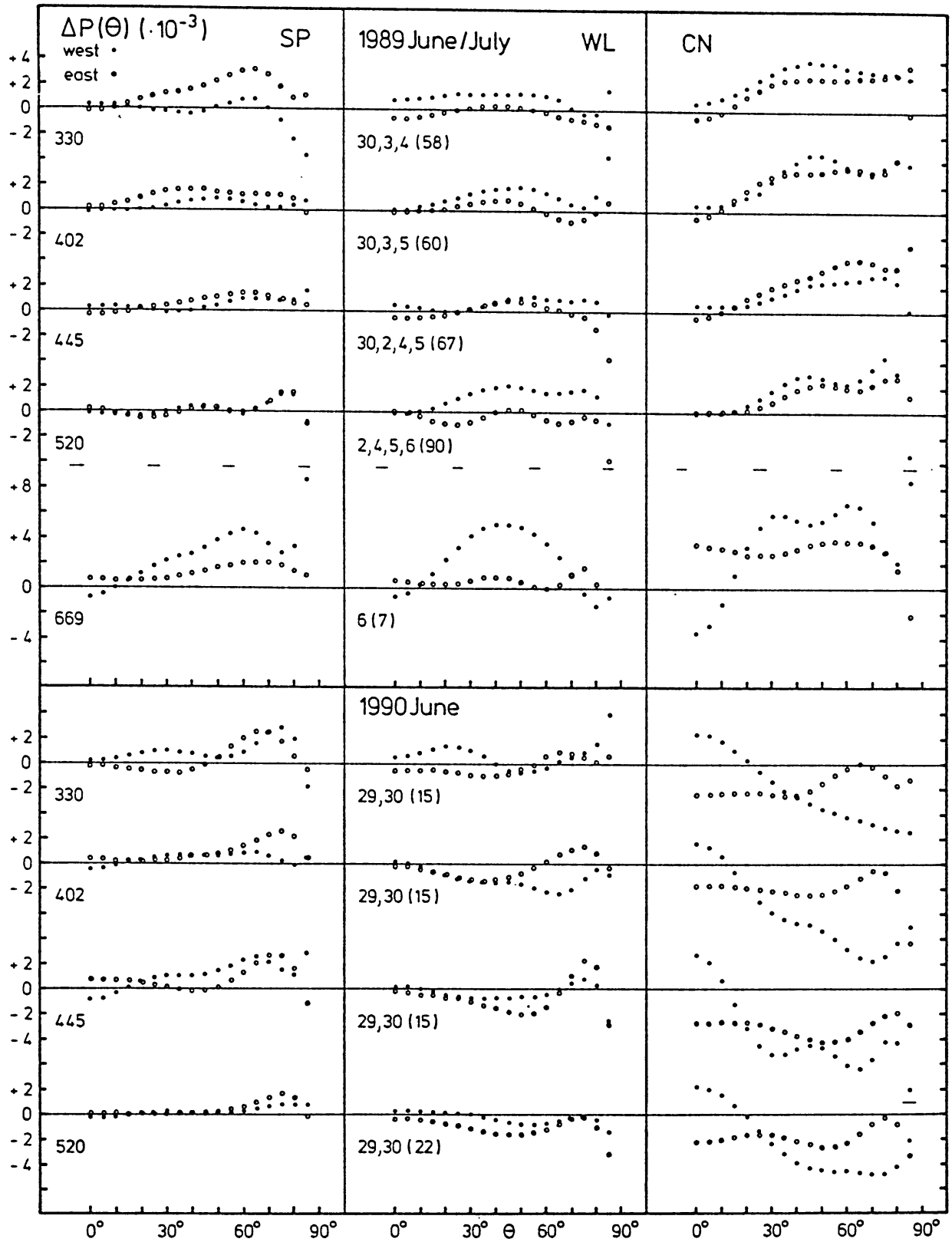

Fig. 6. Differences $\Delta P(\theta)$ between seasonal mean polynomials (west, east) and the reference polynomials. Numbers given for the plots referring to the spectrograph channel (SP) are wavelengths in nm. Plots concerning the WL and CN channels refer to those scans which were obtained simultaneously with the SP scans. The numbers below the WL plots give the day(s) of the month when the observations were made, and (in brackets) the total numbers of scans. The differences are given for every 5°, from $\theta = 0°$ to $\theta = 85°$ ($\sin\theta = 0.996$, $\cos\theta = 0.087$). The plots refer to observing seasons with 'normal' limb darkening (compare Figure 4).

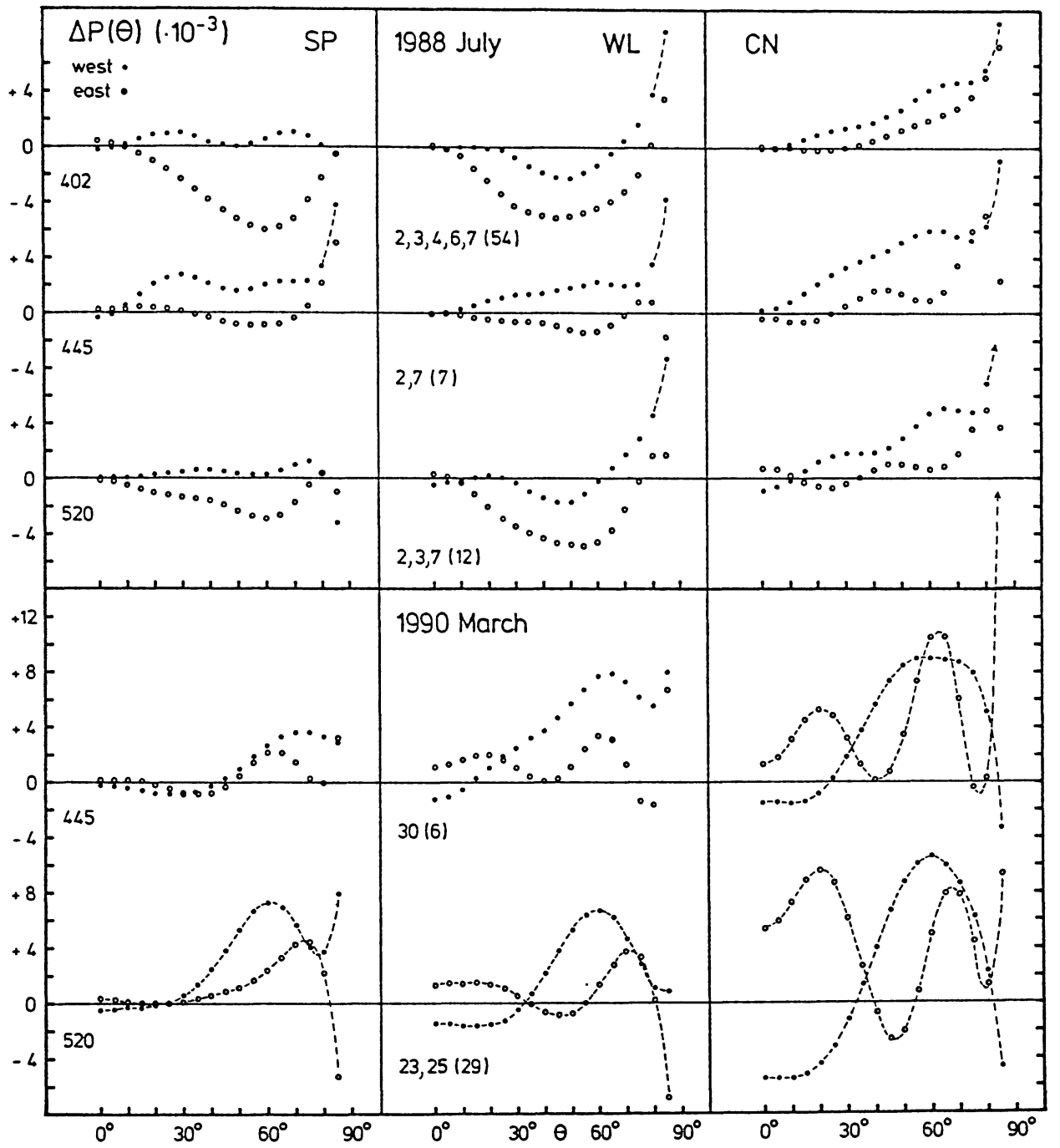

Fig. 7. Differences $\Delta P(\theta)$ between seasonal mean polynomials (west, east) and the reference polynomials as in Figure 6, but for two seasons with 'exceptional' limb darkening (compare Figure 5).

darkening profiles obtained at activity maximum are (almost) as reliable as those obtained at activity minimum. (This is of course confirmed by direct comparisons of the original, observed scans with the resulting polynomials. See also Figure 9.)

Figure 8 represents the one season with a 'very exceptional' limb darkening (in comparison to Figures 6 and 7, the ordinate scales are compressed by a factor 2.5). The plots for $\lambda\lambda 330-520$ nm, which are all averages of more than 50 scans, show for all three channels and for both western and eastern polynomials a very

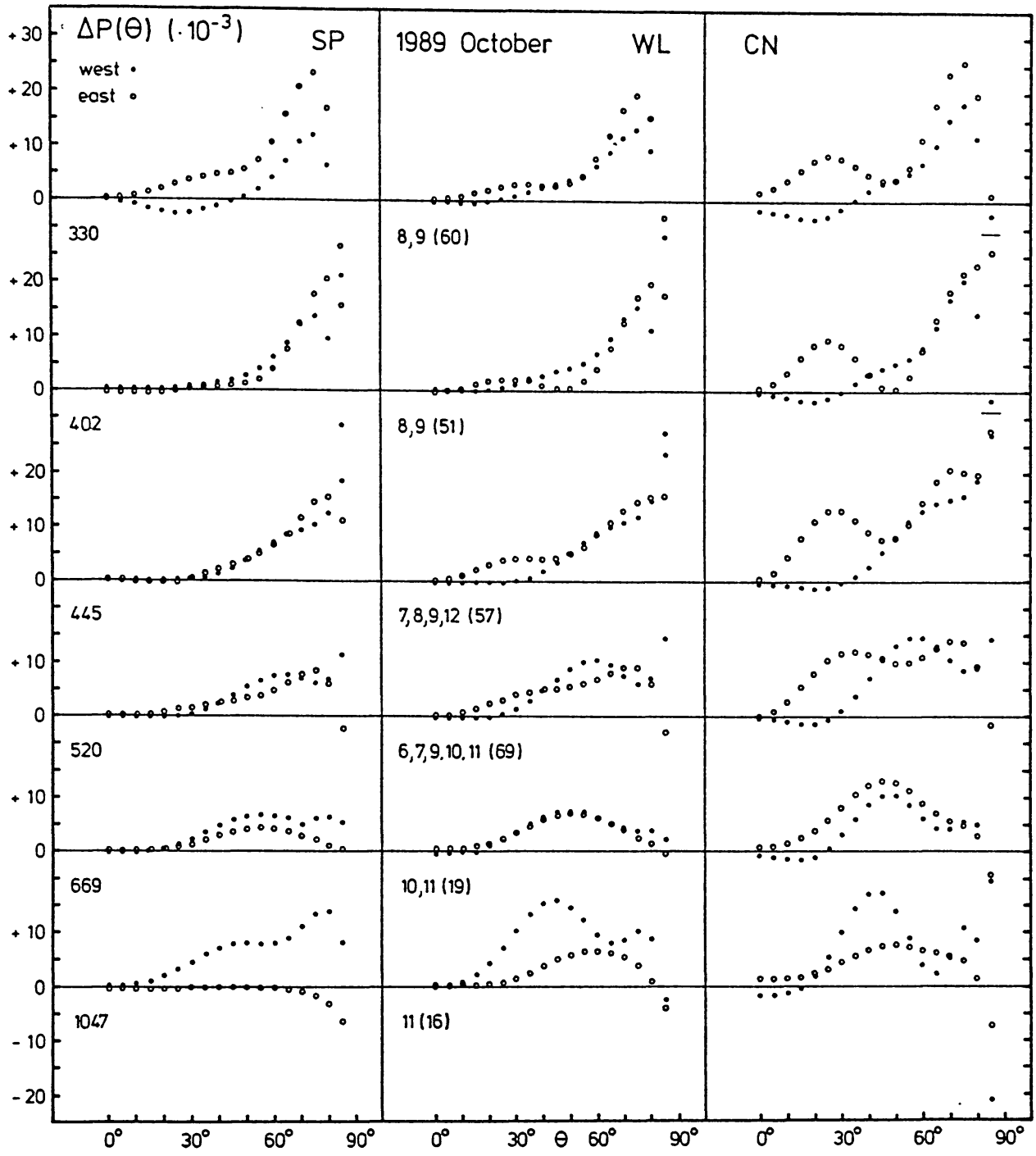

Fig. 8. Differences $\Delta P(\theta)$ between seasonal mean polynomials (west, east) and the reference polynomials as in Figure 6, but for the one season with 'very exceptional' limb darkening (note the different ordinate scales; compare Figure 5).

similar increase towards the limbs. Possibly, this general increase of partly more than 2% reflects a real global enhancement of temperature in the upper photosphere. Significant systematic east–west differences are found only for λ330 nm (east>west), λ669 nm (west>east), and in all CN plots (the CN plots exhibit almost the same wavy structure that can be found in Figure 7 for March 1990). The plot(s)

for $\lambda 669$ nm, which are based on only 16 scans from one single observing day, deviate clearly from the upper plots. This difference illustrates well the selection effects which can become operative if the observations are made on different days and/or the number of scans is not large enough to provide a representative (daily or seasonal) average.

5.2.3. Scan-to-Scan Variations

Figure 9 displays (1) the daily averages of the standard deviations σ_P, which measure the 'scatter' due to the granulation (and possibly to 'remnants' of active regions) and are a by-product of the polynomial fits, and (2) the daily standard deviations $\epsilon_{F/I}$, which refer to the daily F/I averages displayed in Figures 4 and 5. Both data are plotted separately for the western and eastern radii.

Concerning σ_P at *continuum wavelengths* (330–520 nm) we note (1) that it decreases (naturally) with increasing wavelength, (2) that there are no very significant variations from season to season (in the very exceptional season 1989 σ_P was – on average – not larger than it was in the normal season, June 1986). Only in the filter channels, in particular in the CN channel, was σ_P clearly enhanced in both non-summer seasons (1989 October; 1991 March, largest on the second day (25th), when a sunspot group and faculae crossed the observed diameter).

With respect to $\epsilon_{F/I}$ one notices easily that there is no significant dependency on the season, either at continuum wavelengths or in the filter channels. Also a clear dependency on channel or wavelength is not recognizable. Almost independently of time, channel, wavelength, activity, number of averaged scans, and on *the daily average* of F/I (compare, e.g., the east–west differences of F/I with the corresponding differences of the daily means in Figures 4 and 5), $\epsilon_{F/I}$ scatters between 1 and 4×10^{-3}. Obviously, it is just the *daily and seasonal averages* of F/I, which vary with time scales on the order of days, weeks, or even months.

The chaotic and unpredictable manner of the *scan-to-scan* variations is demonstrated in Figure 10, which displays $\Delta F/I$ for all scans of three specific days, separately for all three channels and eastern and western polynomials. These plots are so absolutely typical that we could have selected any other days as well. Actually, we chose the first two days after we had installed the two filter channels, and the last day of the last observing season. It should be noted that the first two days concern an exceptional season with pronounced east–west differences on all days (but being moderate on the first day; compare Figure 5), while the third day refers to a normal season when significant deviations from the reference occurred only in the CN channel (compare Figure 5). It is also worthwhile to identify these days in the plots for σ_P and $\epsilon_{F/I}$ in Figure 9 (N.B.: first two days of '1988 J', last day of '1990 J').

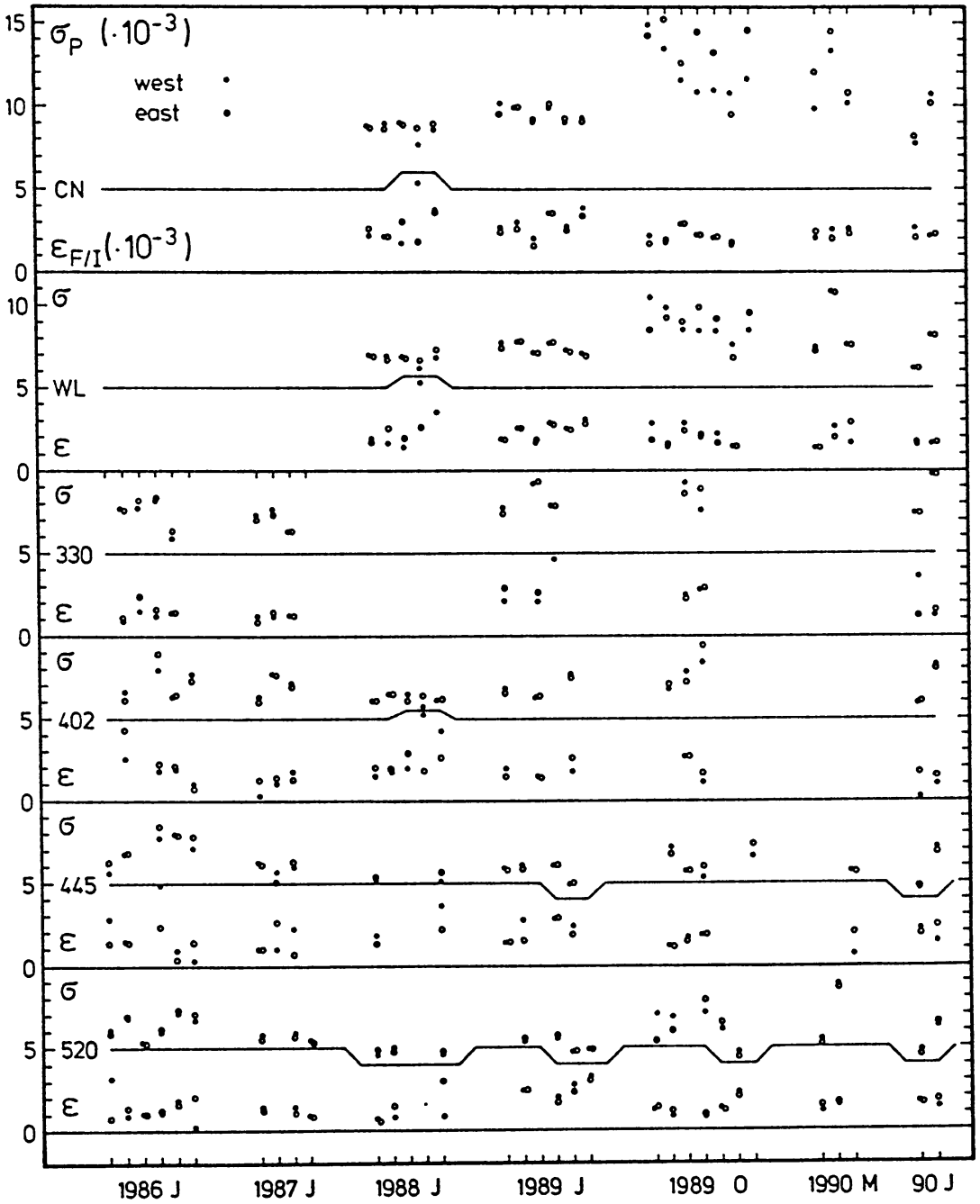

Fig. 9. Daily averages of the standard deviations σ_P resulting from the polynomial fits (mainly due to granulation), and daily standard deviations $\epsilon_{F/I}$ which refer to the daily F/I averages displayed in Figures 4 and 5. Filter channels and continuum wavelengths are identified along the ordinate axis, the observing periods at the bottom. Vertical marks indicate the consecutive observing days.

6. Conclusion

Concerning the solar limb darkening at *continuum wavelengths*, the results of Sections 4 and 5 can be summarized as follows:

(1) The intensity *distribution* across the disk, along the diameter defined by diurnal motion, did not vary systematically from minimum to maximum of the

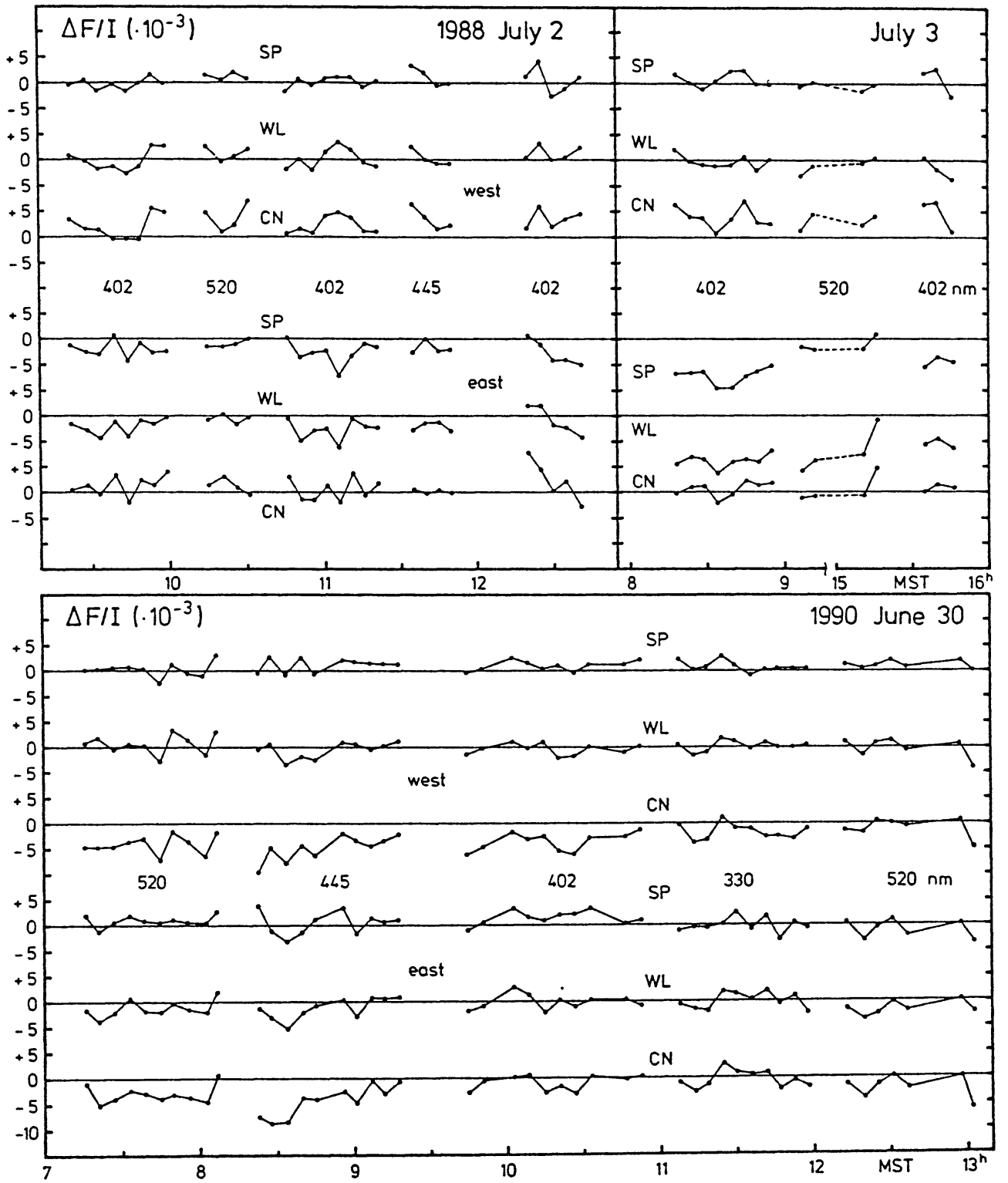

Fig. 10. Scan-to-scan variations of the deviations $\Delta F/I$ from the reference values for three selected days. The plots distinguish eastern and western polynomials and the three channels SP, WL, CN. Numbers are wavelengths in nm (SP channel).

present activity cycle, No. 22. In particular, the *seasonal averages* of the limb-darkening profiles for the four observing seasons June 1986, June 1987, June/July 1989, and June 1990, show a very close agreement (compare Figures 4 and 6).

(2) In the three observing seasons July 1988, October 1989, and March 1990, the seasonal averages of the limb-darkening profiles deviated significantly from the profiles observed in the four other seasons. Furthermore, the day-to-day variations were noticeably larger (Figures 5, 7, and 8). Two of these seasons were at times when the observed diameter crossed the Sun's equator at an angle of about 26°, and met the limbs at corresponding, relatively high, heliocentric latitudes. Nevertheless, this was not the case for the 1988 season, when – moreover – the activity was still at a moderate level and there were no active regions on or near the equator.

(3) In all seven observing seasons the limb-to-limb profiles usually changed from scan-to-scan in a chaotic and unpredictable manner. The size of these variations was almost independent of wavelength. Also dependencies on other quantities (e.g., actual activity level) are not noticeable (Figures 9 and 10).

(4) In most seasons, systematic differences between western and eastern limb-to-limb profiles were very obvious. Such differences concerned either only the wavelengths below 400 nm (Figures 3 and 4) or all observed wavelengths (Figures 5 and 7). The sign of the differences did not usually change within one season. Asymmetries at $\lambda < 400$ nm were in the sense west<east; asymmetries at longer wavelengths had the opposite sign, except for two days in October 1989 (Figures 4 and 5).

(5) The deviations from the adopted reference profiles were usually less than 1% of the disk center intensity, but could occasionally be as large as 3%. In October 1989 the maximum deviations reached 2% even in the seasonal averages.

Similar variations and asymmetries occurred in the two filter channels, but with clear differences in the details. These differences are understandable only if one supposes that all (relevant) variations are of solar origin. This interpretation explains also easily the different scatter in Figure 1 for our final data and the results by Pierce and Slaughter (1977) and Pierce, Slaughter, and Weinberger (1977).

Presumably, most (if not all) of the observed effects, in particular the short-time (scan-to-scan; day-to-day?) variations, reflect just well-known characteristics of the solar photosphere: random fluctuations in distribution, size, and brightness of the granulation, variable structure of the supergranulation network, all sorts of oscillation patterns, minor intensity excesses or deficits connected to active regions. In this respect our results just demonstrate to what extend these solar phenomena can affect 5th-order polynomials which are fitted to the actual intensity distribution. Nevertheless, two characteristics may call for special explanations. (1) The minor, but clearly verified differences between some seasonal overall averages may actually indicate occasional variations of the temperature distribution in the upper photosphere. (2) The small, but also well-established systematic east–west asymmetries may be due to oscillation patterns which could be different on both halves of the solar disk (and have a retrograde rotation? Compare, e.g., Wolff

and Hickey, 1987) or to systematic deviations of the direction of the convection streams from the radial direction (a result of solar rotation or large-scale magnetic fields?).

With respect to other references of limb-darkening variability we refer to our paper on limb-to-limb scans of 20 Å wide spectral bands (Neckel and Labs, 1987).

Acknowledgements

The observations were made when one (H.N.) or both authors were Visiting Astronomers at the National Solar Observatory at Kitt Peak, which is operated by the Association of Universities for Research in Astronomy, Inc., under contract with the National Science Foundation. All observing stays were supported by the Deutsche Forschungsgemeinschaft with travel grants under Ne 91/5.

It is a special pleasure to thank Dr A. K. Pierce for many helpful discussions and suggestions, for his unpublished data on the scattered light at the McMath Solar Telescope (since 1992: McMath–Pierce Solar Telescope Facility), and for reading the first version of the manuscript. Once more we have to thank Buzz Graves for very valuable hints concerning observational details. We also thank Chuck Mahaffey for advising us in using the on-line computer, David Jaksha for providing the basic technical support, and Greg Ladd for managing the final arrangement of all data on magnetic tapes. The hospitality of these and many other staff members of NSO/KPNO made our stays at Kitt Peak at all times enjoyable.

References

Allen, R. G.: 1976, Thesis, University of Arizona, Tucson.

Brückner, G. E., Floyd, L. E., Lean, J. L., Lund, P. A., Prinz, D. K., and Van Hoosier, M. E.: 1994, in J. M. Pap, C. Fröhlich, H. S. Hudson, and S. Solanki (eds.), 'The Sun as a Variable Star', *IAU Colloq.* **143**, Cambridge University Press, in press.

Elste, G. H.: 1990, *Solar Phys.* **126**, 37.

Foukal, P.: 1989, *Solar Phys.* **120**, 249.

Fröhlich, C.: 1994, in J. M. Pap, C. Fröhlich, H. S. Hudson, and S. Solanki (eds.), 'The Sun as a Variable Star', *IAU Colloq.* **143**, Cambridge University Press, in press.

Heath, D. F. and Thekaekara, M. P.: 1977, in O. R. White (ed.), *The Solar Output and Its Variation*, Colorado Assoc. University Press, Boulder, p. 193.

Keenan, P. C.: 1991, *Publ. Astron. Soc. Pacific* **103**, 642.

Neckel, H. and Labs, D.: 1984, *Solar Phys.* **90**, 205.

Neckel, H. and Labs, D.: 1987, *Solar Phys.* **110**, 139.

Neckel, H. and Labs, D.: 1989, *Solar Phys.* **120**, 205.

Neckel, H. and Labs, D.: 1990, *Solar Phys.* **126**, 47.

Pierce, A. K.: 1964, *Applied Optics* **3**, 1337.

Pierce, A. K.: 1990, private communication.

Pierce, A. K. and Slaughter, C. D.: 1977, *Solar Phys.* **51**, 25.

Pierce, A. K., Slaughter, C. D., and Weinberger, D.: 1977, *Solar Phys.* **52**, 179.

Rottman, G., Woods, T. N., White, O. R., and London, J.: 1994, in J. M. Pap, C. Fröhlich, H. S. Hudson, and S. Solanki (eds.), 'The Sun as a Variable Star', *IAU Colloq.* **143**, Cambridge University Press, in press.

Thuillier, G., Simon, P., Herse, M., Labs, D., Gilloray, D., and Petermans, W.: 1994, in J. M. Pap, C. Fröhlich, H. S. Hudson, and S. Solanki (eds.), 'The Sun as a Variable Star', *IAU Colloq.* **143**, Cambridge University Press, in press.
Unsöld, A.: 1955, *Physik der Sternatmosphären*, 2nd ed., Springer-Verlag, Berlin, pp. 613–617.
Wolff, C. L. and Hickey, J. R.: 1987, *Solar Phys.* **109**, 1.